UNIVERSITAT POLITÈCNICA DE CATALUNYA
BARCELONATECH
Escola Superior d'Enginyeries Industrial,
Aeroespacial i Audiovisual de Terrassa

Computational Engineering

CSM: Project

Wing modelling

Master in Aeronautical engineering

Authors:

Alberto Martí, Antoni

Villalta Quintana, Gerard

Professor:

Cante Teran, Juan Carlos

Date:

January 10^{th}, 2023

Table of Contents

List of Figures

List of Tables

1 Problem Description

The present project aims to study a wing prototype with a NACA0018 airfoil. The wing structure is composed of an outer skin, a set of ribs, two main spars and a range of stringers. All these elements' location on the structure and its properties can be seen in figure 1. The wing is mounted in a wind tunnel, with its root section fixed. All this root nodes will have their degrees of freedom set to 0. Next the different loads that the structure is subjected to will be explained.

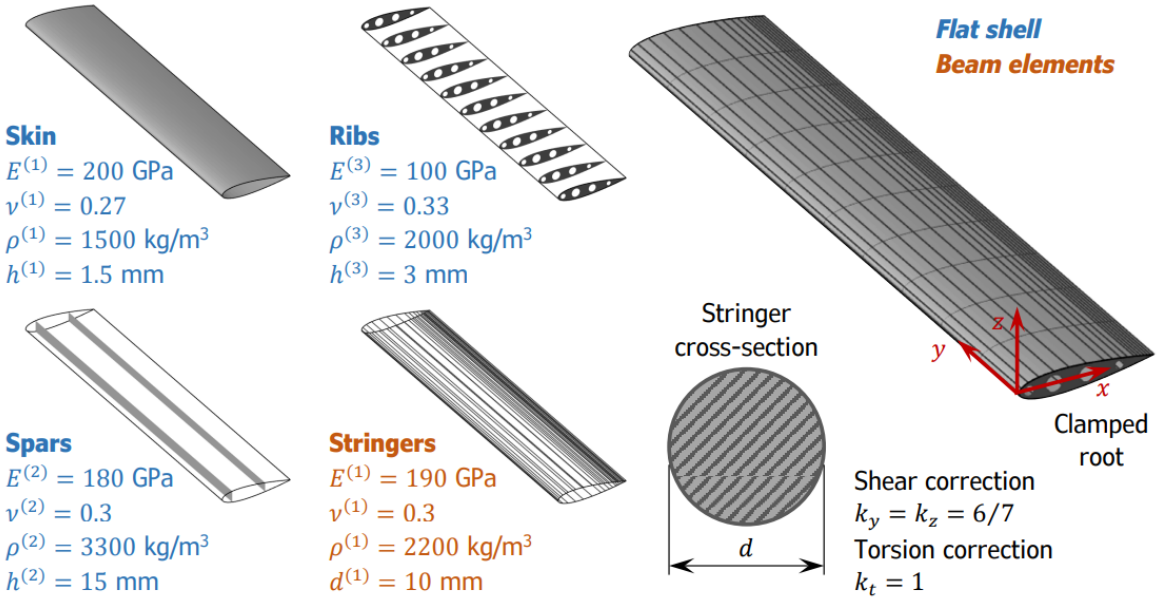

FIGURE 1: Wing geometry and materials

1.1 Aerodynamic pressure loads

The main load that the wing will be subjected to are the pressure loads produced by the fluid moving around the outer skin of the wing. The pressure distribution over the wing is defined by the equation 1 for the suction side of the wing and equation 2 for the pressure side. An example distribution of the pressure around the airfoil section can be seen in figure 2.

$$p_u(x,y) = -4\alpha P(y)\left[\left(1-\frac{x}{c}\right)^4 + \sqrt{1-\frac{x}{c}}\right] \tag{1}$$

$$p_l(x,y) = 4\alpha P(y)\left[\left(1-\frac{x}{c}\right)^4 - \frac{1}{4}\sqrt{1-\frac{x}{c}}\right] \tag{2}$$

$$P(y) = \begin{cases} p_\infty & for \;\; y \leq 0.8b \\ p_\infty \cos\left(\frac{\pi}{2}\frac{y-0.8b}{0.2b}\right) & for \;\; y > 0.8b \end{cases} \tag{3}$$

This two equations (1 and 2) define the pressure on point on the surface of the wing in function of the chord (c), the location along the chord (x), the angle of attack (α) and $P(y)$. This last is defined in equation 3 and is proportional to the dynamic pressure of the free stream (p_∞) and

it depends on the location along the span of the wing and the own value of the span of the wing (b).

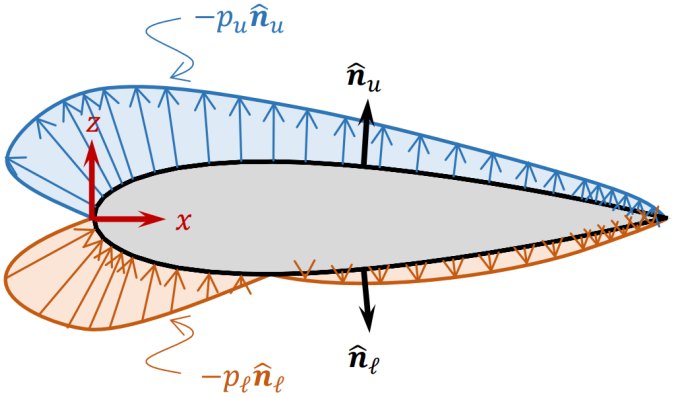

FIGURE 2: Airfoil's pressure distribution schematic

The pressure obtained with the previous equations is the one normal to the surface of the outer skin. Also, the pressure calculated is the pressure of the fluid and not the pressure over the skin. Then, to compute the distributed force along the outer skin of the wing, it is required to compute the reaction over the surface (adding a minus sign) and expressing the pressure in its respective components.

1.2 Mass matrix and body forces

For this study, the mass of the structure is also considered for the static analysis. To do so, a value of acceleration, in this case the Earth's gravity (g), is defined for every node of the model. This acceleration is then multiplied by the elements' mass and the resulting force added to the force vector, which will be fully determined by this loads and the aerodynamic pressure loads.

In addition, the mass matrix M is also required to perform the modal analysis and to compute the natural vibration modes. This natural modes are later used to perform the model order reduction.

The different elements related to each of the part of the wing will have their corresponding value of density and will be subjected to the same constant value of gravity.

1.3 Wing's structural and material properties

As it can be seen in figure 1, each part of the wing is made of different materials with different properties. The basic elastic parameters of each material (Young's modulus and Poisson's coefficient) are stored in a material matrix that relates each material to an specific ID. The same is done for the values of density and section size (thickness of plate and diameter of beam).

The structural theories used to solve this model are the previously studied Timoshenko 3D Beams and Flat Plate theory. Added to the hypothesis that arise from this two theories, the small strains hypothesis is also applied to model the structural response inside the linear elastic regime.

The implementation of the previously mentioned theories imply the definition of some shear and torsion correction parameters that adjust the results to a more realistic outcome. In this case, the already presented values in figure 1 apply for the beam elements and the shear correction factor $K_s = 5/6$ is defined for shell elements.

2 Results

In this section the results of the performed study will be discussed. In total, three studies have been carried out. First the study of the static response of the structure under the specified angle of attack and free stream dynamic pressure (q_∞), that are shown in table **??**. To compute the

2.1 Complete static solution

The static solution provides the expected stresses and strains that the model would have under certain boundary conditions. In our case, the wing model is clamped from the root of the wing (cantilever) and subject to its own weight and aerodynamic forces.

The global algorithm used to solve the static response of the problem is the following:

1. Define all parameters and compute the boundary conditions matrices (U_p,B_e,P_e)
2. Compute K_{beam}, M_{beam} and F_{beam} using Timoshenko theory
3. Compute K_{shell}, M_{shell} and F_{shell} using Flat Plate theory
4. Apply the B.C. restrictions over the displacement vector (I_f,I_p)
5. Add all beam and shell matrices:

$$\hat{K} = K_{beam} + K_{shell}$$
$$\hat{M} = M_{beam} + M_{shell}$$
$$\hat{f} = f_{beam} + f_{shell}$$

6. Solve the matrix system and obtain displacements and reactions:

$$\hat{u}(If,1) = [\bar{K}(If,If)]^{-1}(\hat{f}(If,1) - [\hat{K}(If,Ip)]\hat{u}(Ip,1)) \tag{4}$$

7. Compute the Von Mises stresses for shell elements

Following the previous steps with the parameters in table 1, the first results we can obtain is the correct implementation of the pressure distribution along the chord. In figure 3, suction and pressure sides of two wing sections are plotted.

TABLE 1: Wing initial parameters

α [°]	α[rad]	**c**[**m**]	**b**[**m**]	$\mathbf{p}_\infty$[**Pa**]	**g** [m/s^2]
10	$\pi/18$	0.6	3	$1.5625 \cdot 10^5$	-9.81

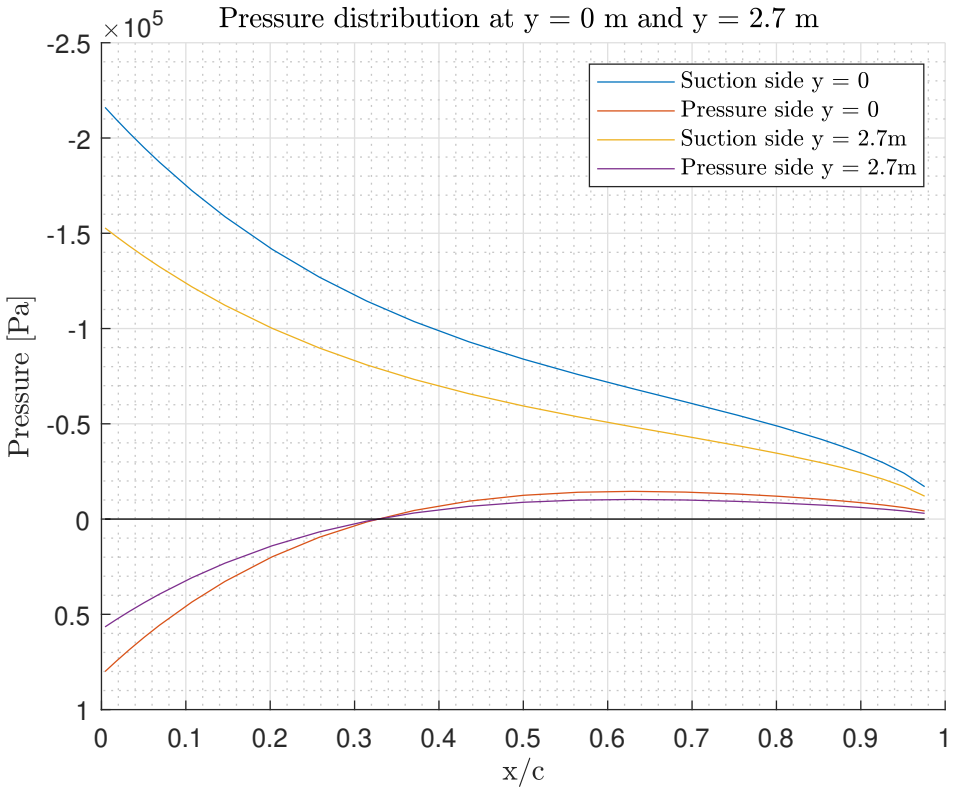

FIGURE 3: Pressure distribution at the root and near the tip

With the aerodynamic parameters shown in table 1, the wing experiences a constant pressure distribution up to $y = 0.8b$ and then it reduces to a 0 pressure distribution at the tip. A representation of the pressure over the two locations along the span (at $y = 0m$ and $y = 2.7m$) can be seen in figure 3. The pressure shown correspond to the normal to the surface of the airfoil, so to compute the the total pressure acting in the vertical direction, the decomposition of the pressure should be carried out.

The final static response and Von Mises stresses can be found in figure 4.

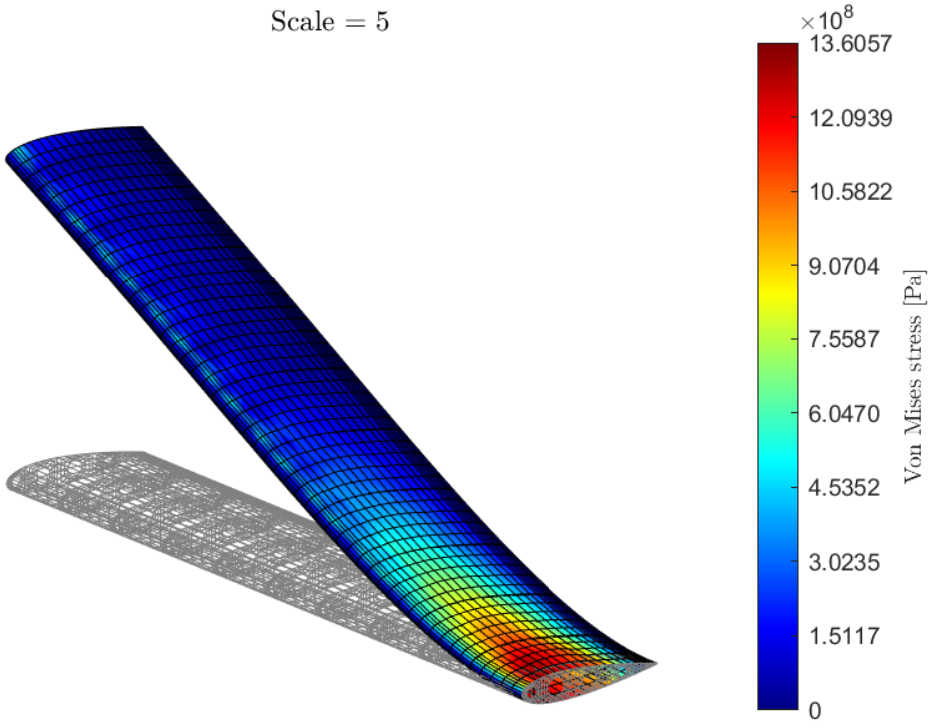

FIGURE 4: Static deformation of the structure

As expected, the results obtained have some similarities with any typical cantilever problem. Due to the positive deflection of the wing, it can be clearly stated that the aerodynamic forces are more predominant that the wing's mass forces. This deflection has a maximum value at the tip of 0.24 m.

In addition, the maximum stresses can be found at the root, where the maximum bending moment appears (commonly the dominating one). This value is approximately 1.36 GPa. Nevertheless, in the leading edge also appear certain stresses because it is the region of the airfoil with highest pressures (see figure 3). Some variations can be seen depending on the location of the internal ribs and the bending moment at each wingspan position.

From an structural point of view, the maximum stresses obtained could not be resisted by almost any material. Thus, a first approach could be to increase the thickness and diameter of the elements. Another solution could be to reinforce the upper and lower skin shells and distribute the stresses alogn the wing.

2.2 Modal analysis

To perform the modal analysis of the structure, two matrices are required, the stiffness matrix K and the mass matrix M. The process to obtain this two has already been explained in the previous section 2.1. This two matrices define the system of equations shown in expression 5, that is an eigenvalues problem. By obtaining the eigenvalues (λ_j) and eigenvectors ($\{\hat{\Phi}_j\}$) of the system, the natural modes of vibration of the structure will be obtained.

$$([K] - \lambda_j[M])\{\hat{\Phi}_j\} \tag{5}$$

Using the function *eigs* from *MATLAB*, the first 12 mode shapes have been computed. After the mass normalising the mode shapes as and computing the frequencies from the eigenvalues ($\omega_j^2 = \lambda_j$). This results are shown **??** and the frequencies are collected in table 2.

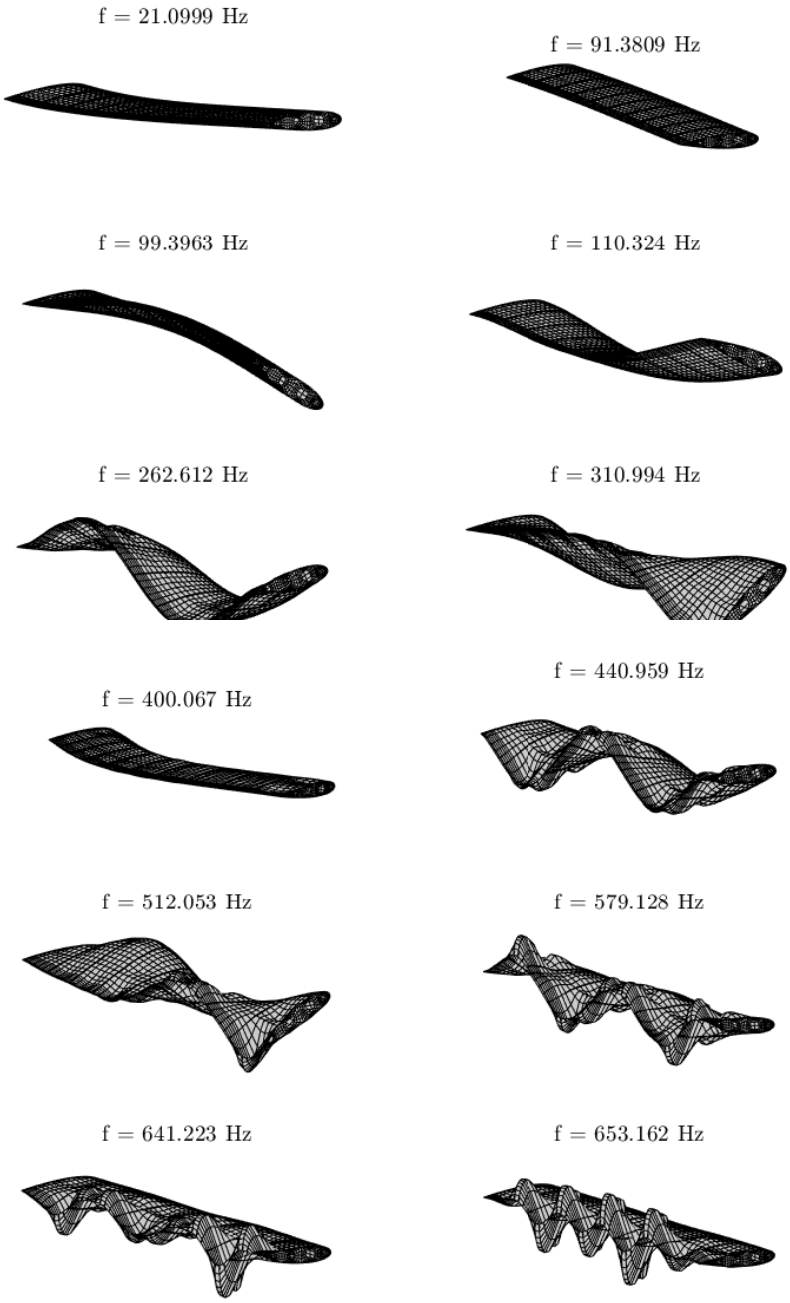

FIGURE 5: First 12 natural vibration modes

TABLE 2: Natural frequencies of the first 12 mode shapes

Mode	**Freq [hz]**
1	21.10
2	91.38
3	99.40
4	110.324
5	262.61
6	310.99
7	400.07
8	440.96
9	512.05
10	579.13
11	641.22
12	653.16

Comparing the computed mode shapes from figure 5 with the modes that appear in a common benchmark problem of a cantilever (see figure 6), clear similarities can be seen between some of the modes:

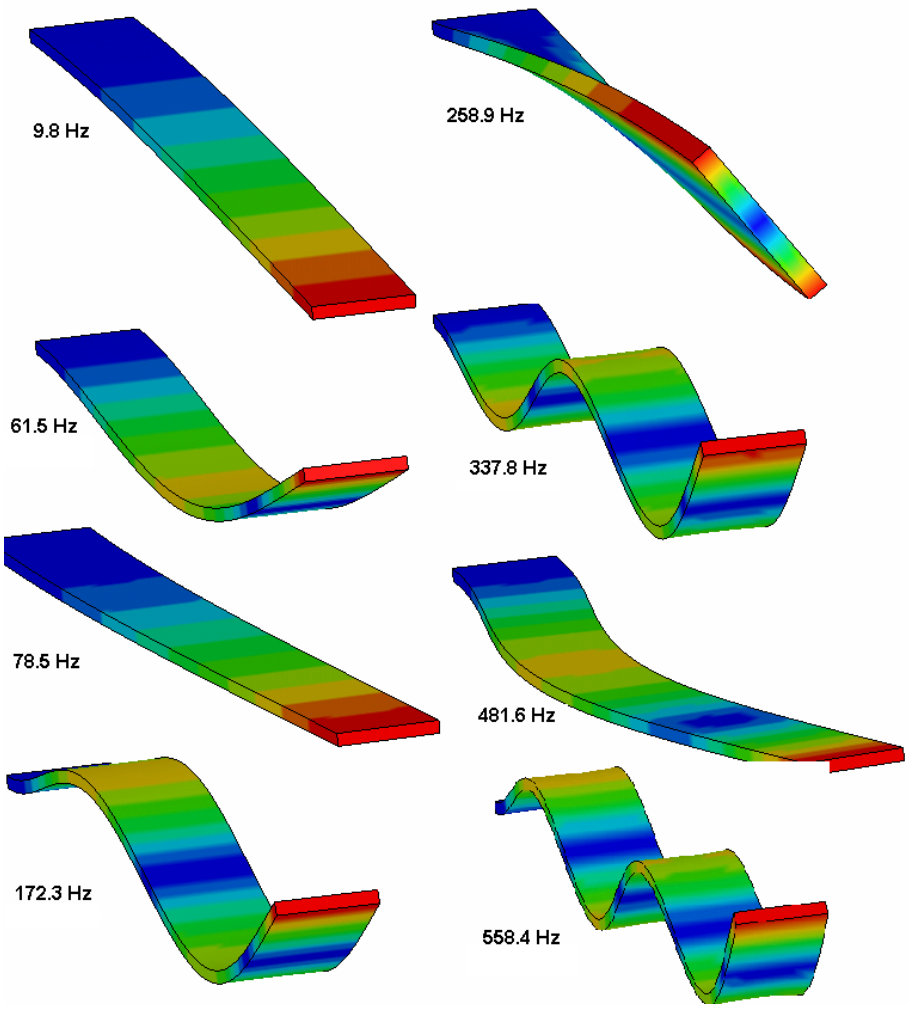

FIGURE 6: Natural response of a cantilever [1]

In both cases, modal shapes purely related to bending, stretching and torsion appear. The flapping responses computed 1,4,5 and 8 clearly match with the modes 1,2,4 and 6, both corresponding to standing waves with increasing number of nodes. Moreover, the stretching mode number 2 is the same as the 3rd one of the cantilever and the torsion mode number 6 is clearly related to the cantilever 5th mode. The different order of the modes and the existence of modes with combinations of excitations obtained is clearly caused by the higher complexity of our model.

Regarding the obtained results, it can be seen how the first mode corresponds to a flapping motion, the second mode a plunge, the third one is a combination of torsion and flapping and the fourth one is also a combination of torsion and flapping, but the wing has to inflection points, at the root and at half span. These 4 first modes obtained would be the most critical modes of the structure as they present relatively low frequencies, with the first one being very low at just 21 Hz. This first mode could probably be started by a turbulence in the air stream that induced a sudden loss of lift and could initiate fluttering of the wing. For a possible improvement of the wing prototype, it would be interesting to try to have this first mode frequency as high as possible for obvious safety reasons.

2.3 Model order reduction

The model order reduction is a technique that allows to compute the response of the structure to oscillatory loads, but also to static ones (by setting the frequency $\omega = 0$). The way this process works is by using the a finite set of natural modes of vibration and projecting them to the system. However, to be able to perform this process, first it is required to perform a model analysis to obtain the most relevant modes (the lowest frequency ones first) and their respective eigenvectors and eigenvalues. For this assignment, this has already been done in the section 2.2 and the first 12 modes have been computed, more than the ones required for the next study. For this section, it will be compared the solution obtained in the section 1 where the displacements have been calculated using expression 4 against the one obtained with the projection of just the 2 first modes and the 6 first modes for a frequency $\omega = 0$.

The general algorithm to perform the model order reduction is described next:

1. Select the modes to project the system I_m
2. Define the approximated displacement vector U^*
3. For mode j in I_m, compute the modal amplitude $\alpha(j)$
4. Add the mode j's to the approximated displacement vector U^*
5. Go to next mode in I_m ($j = j + 1$). Else, go to next step
6. Obtain the approximated displacements of the structure U^*

The deformed structures for the projection using 2 modes is shown in figure 7 and for 6 modes in figure 8. Several are the differences that can be seen just by looking at the deformed structures. First of all, the maximum stress of the outer skins at the root is is higher in the model reduction than in the static case (as can be seen in figure 4). However, looking in more detail at the Von Mises tension near the root it looks like that are has lower tension than in the static solution. Regarding the deformed structure shape, the the two mentioned figures it can be seen how the solution model reduction solution with just 2 modes presents a negative twist at the tip that is not present in the 6 mode solution and the static solution.

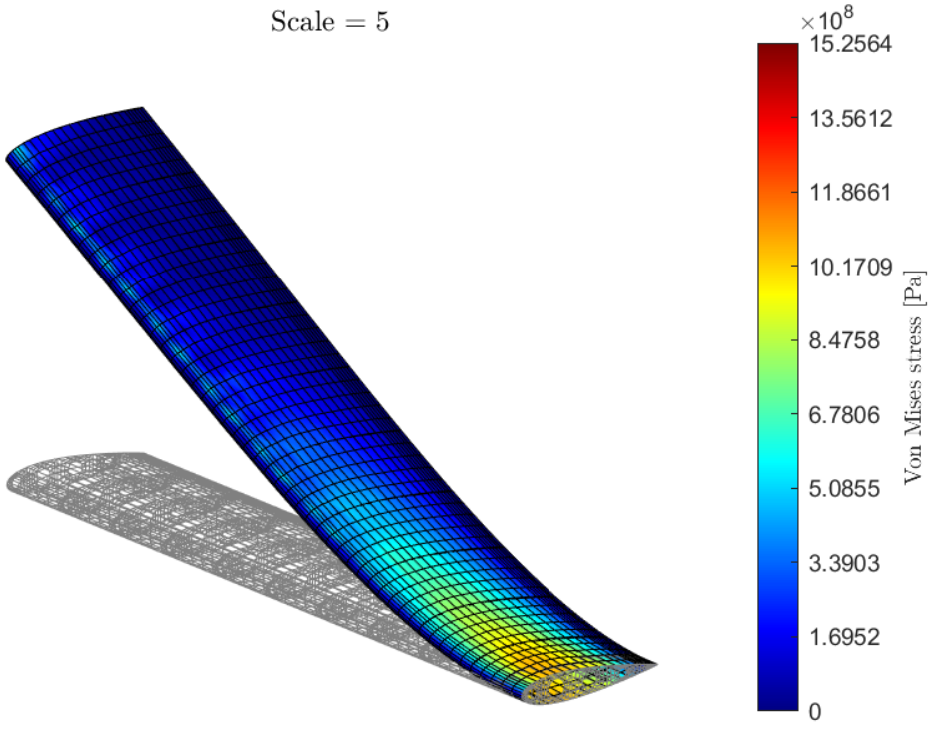

FIGURE 7: Static deformation of the structure applying the modal order reduction with the first 2 modes

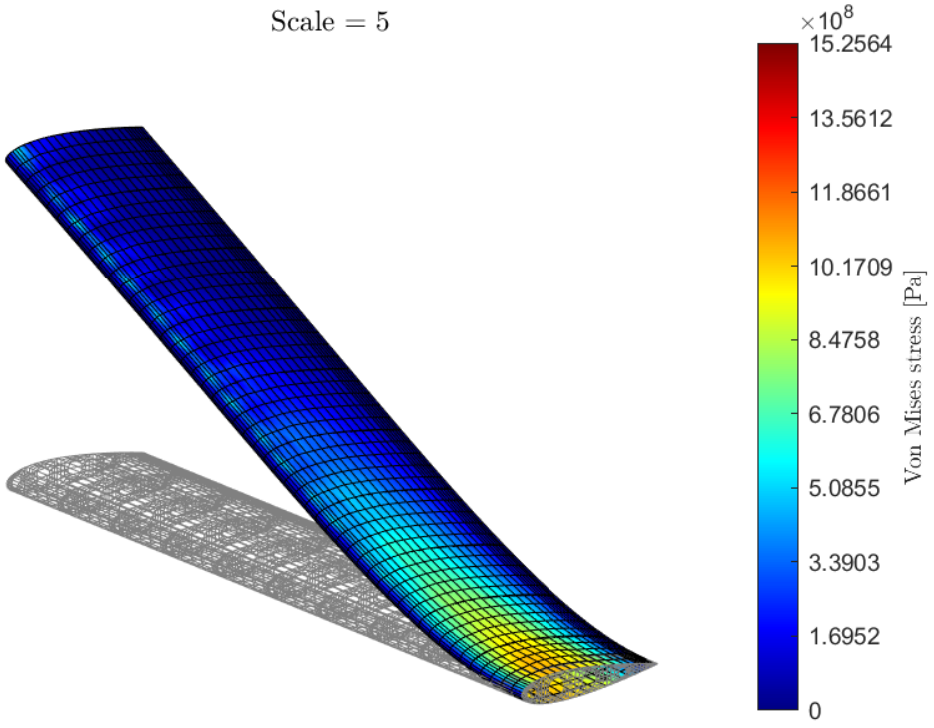

FIGURE 8: Static deformation of the structure applying the modal order reduction with the first 6 modes

To better assess the differences between the static solution and the two from the model order

reduction, the vertical displacement of the leading edge (figure 9) and the trailing edge (figure 10) have been plotted along the span-wise direction. As can be seen in figure 9 the model reduction with only 6 modes is already matching very well the solution of the static case. However, the the one with 2 modes presents some differences at the mid span location, having smaller displacement than in the other solutions, but is matching well the tip displacement. For the trailing edge, the differences are greater. The 2 mode solution presents a higher displacement on the tip than the other two solutions, what explains the noticeable twist observed in the deformed structure. In table 3 this results and the ones corresponding to the highest tension are collected.

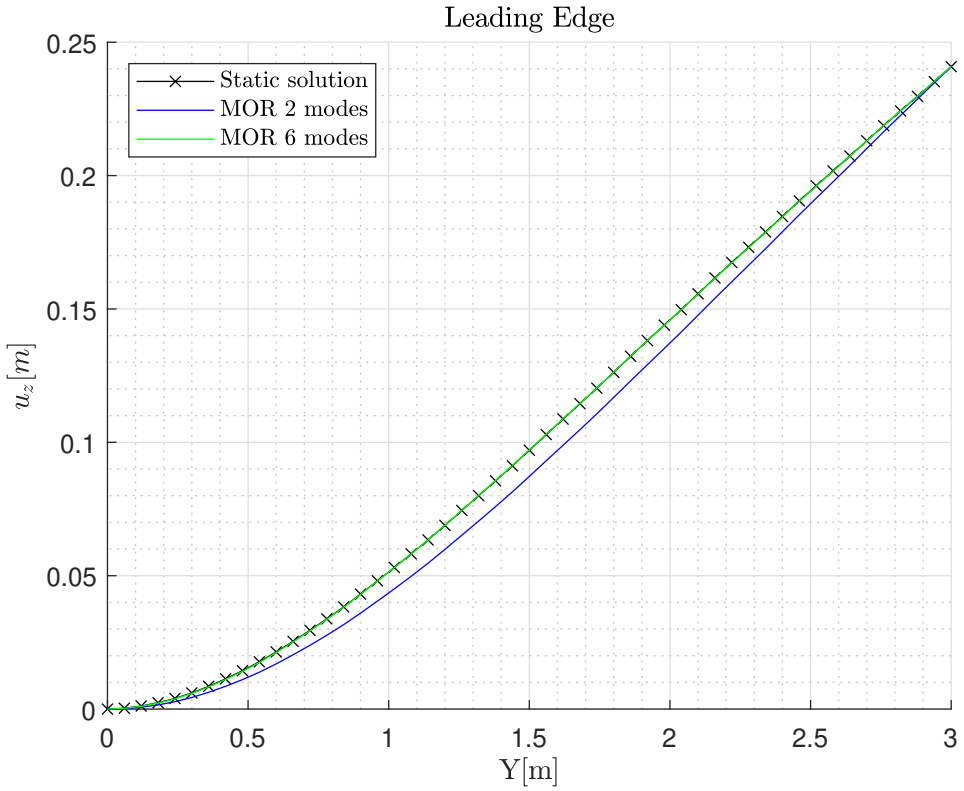

FIGURE 9: Leading edge vertical displacement

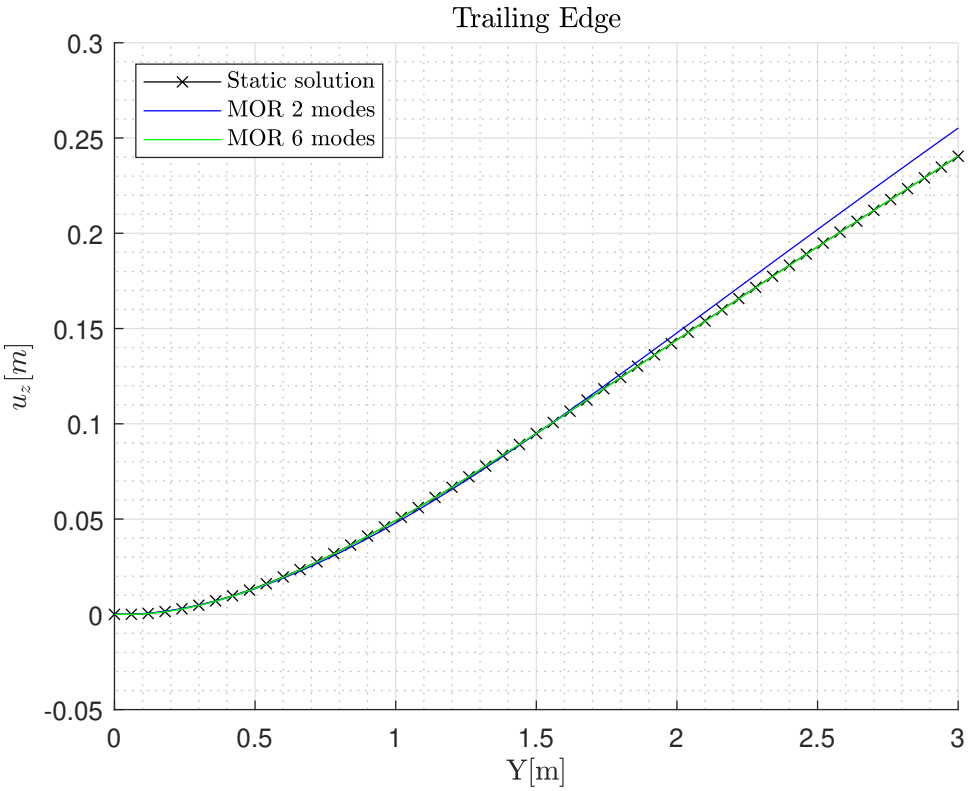

FIGURE 10: Trailing edge vertical displacement

TABLE 3: Differences between the static solution and the ones with the Model order reduction

	Static solution	**MOR with 2 modes**	**MOR with 2 modes**
u_z^{tip} **at the LE [mm]**	240.84	241.00	240.94
u_z^{tip} **at the TE [mm]**	240.43	255.21	240.59
Max stress [Pa]	13.61E+08	15.26E+08	15.26E+08

Even if the solutions computed with the model order reduction are not totally precise, they have the same order of magnitude as the solutions obtained by solving the complete system. Nevertheless, the main advantage of this method is the reduced cost required to get accurate results with a low computational power. To apply this method it is necessary to assemble the both stiffness and mass matrices, that is costly, and to perform a modal analysis to obtain the mode shapes, that is also costly. However, as long as the structural model doesn't change, this operations have to be performed only once and with this results and the model reduction many loads can be applied to the structure, even test the frequency response of this one. Then the advantages are clear.

3 Conclusions

After performing the structural analysis of the proposed wing, it can be considered that the results obtained match the expected results compared to some simpler benchmark problems.

The results of the static analysis are very similar to a basic cantilever problem, which normally presents a maximum deflection at the tip and maximum stress at the root due to the maximum bending moment. In our case, the maximum positive deflection of 0.24 m show that the aerodynamic forces surpass the weight ones. Those forces generate great stresses near the root, with a maximum value of 1.36 GPa. This value is inadmissible for any metallic material commonly used in the aerospace industry. A first approach to solve this problem is to increase the thickness and section of the different elements.

The modal analysis performed also show clear similarities with the natural responses of a benchmark cantilever. Among the 6 first modes, they appear modes clearly related to bending (1,5) stretching (2) and torsion (6). Due to the complexity of the model, other natural responses appear which are combinations or excite certain specific parts of the wing. Nevertheless, those modes require higher amounts of energy to be developed.

Finally, after computing the displacement using the model order reduction, the advantages of this method clear. Just by using 6 modes, the accuracy of the displacements compared to the complete solution is very high. However, the computed stresses are higher than the ones of the complete model, and they are don't present the same distribution over wing surface. Even with the difference in stress results, this method shows to give accurate structural models with a low computational cost.

References

1. KARPANAN, Kumarswamy. Experimental and numerical analysis of structures with bolted joints subjected to impact load. 2023-01.